Electronic Supplementary Information

$FeCo_2O_4$ submicron-tube arrays grown on Ni foam as high rate-capability and cycling-stability electrodes allowing superior energy and power densities with symmetric supercapacitors

Baogang Zhu,‡ Shaochun Tang,*‡ Sascha Vongehr, Hao Xie, Jian Zhu, Xiangkang Meng*

National Laboratory of Solid State Microstructures, College of Engineering Applied Sciences and Institute of Materials Engineering, Nanjing University, Nanjing 210093, Jiangsu, P. R. China

Corresponding authors

* Tel.: (+86)-25-83685585; Fax: (+86)-25-83595535;

Correspondence and requests for materials should be addressed to S.C. Tang (tangsc@nju.edu.cn) or X.K. Meng (mengxk@nju.edu.cn).

1. Experimental section

2. Figures and figure captions

Fig. S1. The tubes before thermal treatment: (a) SEM images, (b) low- and (c) high-magnification TEM, and (e) HRTEM images.

Fig. S2. XPS spectra of the $FeCo_2O_4$ on Ni foam.

Fig. S3. SEM images of the $FeCo_2O_4$ grown on Ni foam obtained with different C_{Fe}^{3+} of (a) 1.3 mM (b) 5.0 mM (c) 12.5 mM (d) 17.5 mM.

Fig. S4. TGA curve of a typical sample before thermal conversion, which was recorded from room temperature to 600°C.

Fig. S5. SEM image (a) and CV curves (b) of typical $FeCo_2O_4$ tube arrays on Ni foam after ultrasound.

Table S1. Comparison of the optimal $FeCo_2O_4$ submicron tubes on Ni foam and previously reported ternary metal oxides of cobalt

1. Experimental section

Synthesis. All reagents were analytical grade and used without further purification. 0.71g of $Fe(NO_3)_3 \bullet 9H_2O$ and 1.02 g of $Co(NO_3)_2 \bullet 6H_2O$ were dispersed in 50 mL of deionized water. This solution was transferred into a 250 mL three-necked flask with cleaned nickel foam and heated to 80 °C. Then, 2.65g of oxalic acid was dissolved in 50 mL of deionized water and then slowly injected into the flask. The thus resulting concentrations of Fe^{3+}, Co^{2+}, and oxalic acid were 17.5, 35, and 210 mM, respectively. The concentration of all reactants was changed together by diluting all solutions (C_{Fe}^{3+} values are 12.5, 10, 5 and 1.25 mM). This ensures the desired stocheometric ratios and provides one single parameter (the size of the three coupled concentrations) that can be systematically changed. The reaction system was kept at 80 °C for 2 h under mechanical agitation and then cooled to room temperature naturally. The product was collected, washed with deionized water, freeze-dried, and annealed in air at 400 °C for 2 h.

Materials characterizations. Powder X-ray diffraction (XRD) with a D/Max-RA X-ray diffractometer (Cu Ka =1.5418 A radiation) at 5° min^{-1} characterized crystal structure and chemical compositions. Scanning electron microscopy (SEM) images were obtained on a field emission scanning electron microscopy (FE-SEM) on S-4800 (Hitachi) at 10 kV. Transmission electron microscopy (TEM), HRTEM, and selected area electron diffraction (SAED) were analyzed on a JEM-2100 (JEOL) at an acceleration voltage of 200 kV. X-ray photoelectron spectroscopy (XPS) examined the valence states of elements in a Thermo VG Scientific MultiLab ESCA2000 system with a CLAM4 hemispherical analyzer at a base pressure below 3×10^{-10} mbar. Thermogravimetric

analysis (TGA) was performed on a TGA/SDTA thermogravimetric analyzer from room temperature to 600°C in air at a heating rate of 20 °C min^{-1}.

Electrochemical measurements. The electrochemical performance was evaluated with a typical three-electrode system on a Metrohm Autolab 302N electrochemical workstation at room temperature in 3 M KOH aqueous solution. The $FeCo_2O_4$ on Ni foam (2 cm × 1 cm) was used as the working electrode; a platinum plate served as counter electrode and a Ag/AgCl reference electrode was used. Cyclic voltammetry (CV) scans were measured between -0.2 and 0.6 V at various scan rates. Galvanostatic charge–discharge (CD) cycle tests were investigated in the range of zero to 0.6 V at various current densities. Specific capacitances were calculated from the galvanostatic CD curves. Specific areal capacitances (C_a) were calculated using $C_a = I\,\Delta t/(S\,\Delta V)$, where I is the applied current, ΔV is the selected, linear voltage drop, Δt is the corresponding discharge time, and S is the area of the electrode (S = length × width). I/S is the current density and $\Delta V/\Delta t$ is the slope of the discharge along the selected linear region. For the electrode obtained at C_{Fe}^{3+} = 10 mM observed with a current density of 2 mA/cm^2 (see blue line in Fig. 3b), the most linear discharge voltage drop range extends from 0.55 to 0.4 V with the corresponding Δt being from 415 s to 556 s. Therefore, C_a = 2 mA/cm^2 × 141 s/ 0.15 V = 1.88 F/cm^2. In the same way, at 4, 10, 20, 40 and 100 mA/cm^2 (Fig. 4b), the C_a are 1.78, 1.64, 1.56, 1.46 and 1.38 F/cm^2, respectively. The corresponding gravimetric capacitances are $C_g = I\,\Delta t/(m\,\Delta V)$, where m is the mass of the active material, and other parameters are the same as above, thus $C_g = S \times C_a/m$. For example, at 4 mA /cm^2, the mass density m/S = 1.5 mg/cm^2 (obtained from TGA) leads to C_g = 1186 F/g.

The electrical impedance spectroscopy (EIS) was tested in the range from 100 kHz to 0.1 Hz with an AC amplitude of 5 mV. Cycling life was investigated on a Land Battery Test System (Wuhan Kingnuo Electronic Company, China). The anode was the $FeCo_2O_4$/Ni foam electrode, and the cathode was blank nickel foam.

All-solid-state symmetric supercapacitors were assembled with PVA/KOH as separator and electrolyte between two $FeCo_2O_4$ electrodes. PVA/KOH composite gel electrolyte was prepared by mixing PVA powder (1.5 g), KOH (1 g), and deionized water (18 mL) under a vigorous stir at 95 °C until the solution became homogeneous. The CV scans were investigated between 0-1 V at various scan rates. CD testing was performed from 0-0.7 V at various current densities. Energy density (E) was calculated using $0.5\ C_s\ \Delta V^2$. Power density (P) was calculated via $P = E/\Delta t$.

2. Figures and figure captions

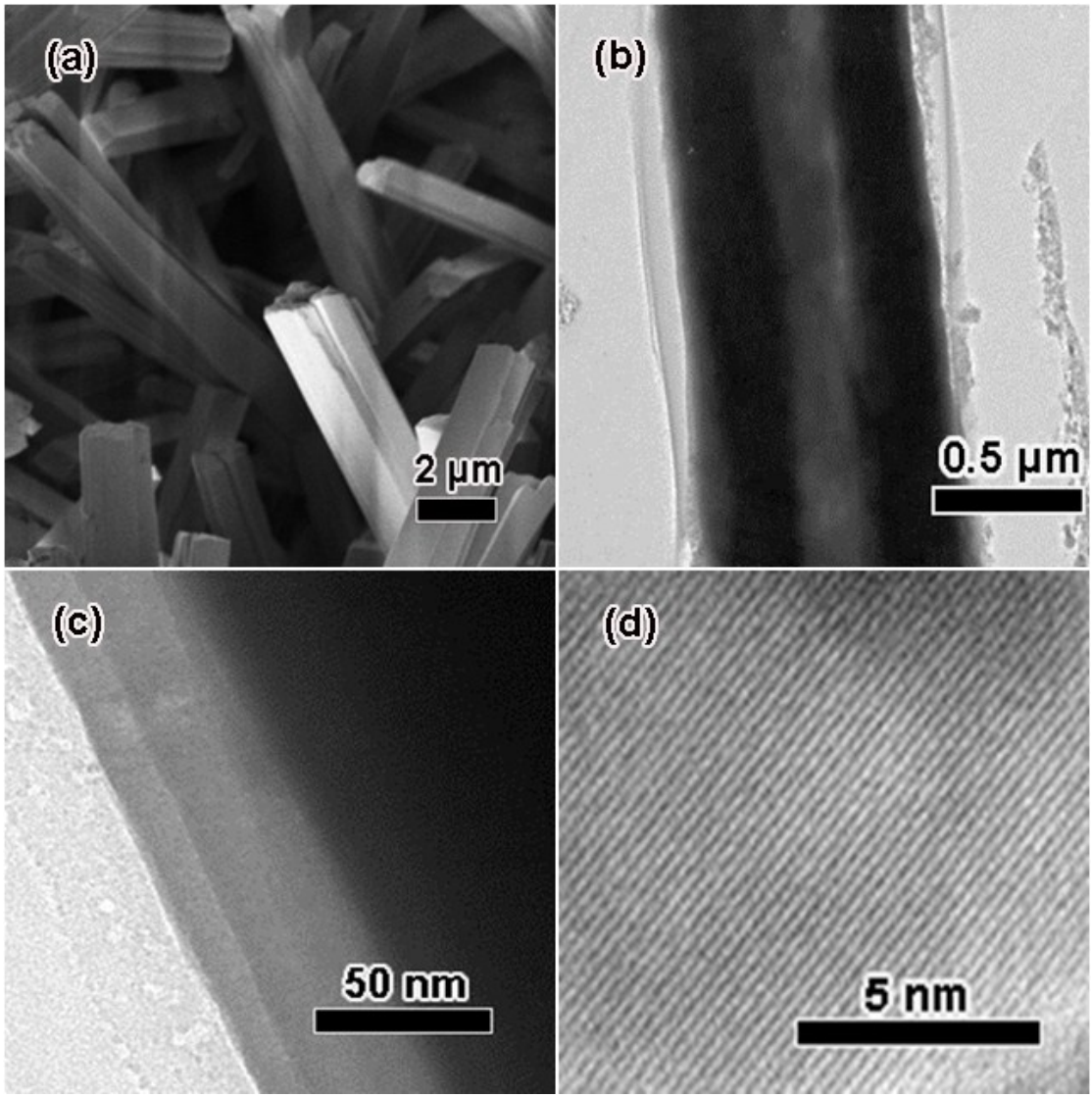

Fig. S1. The tubes before thermal treatment: (a) SEM images, (b) low- and (c) high-magnification TEM, and (e) HRTEM images

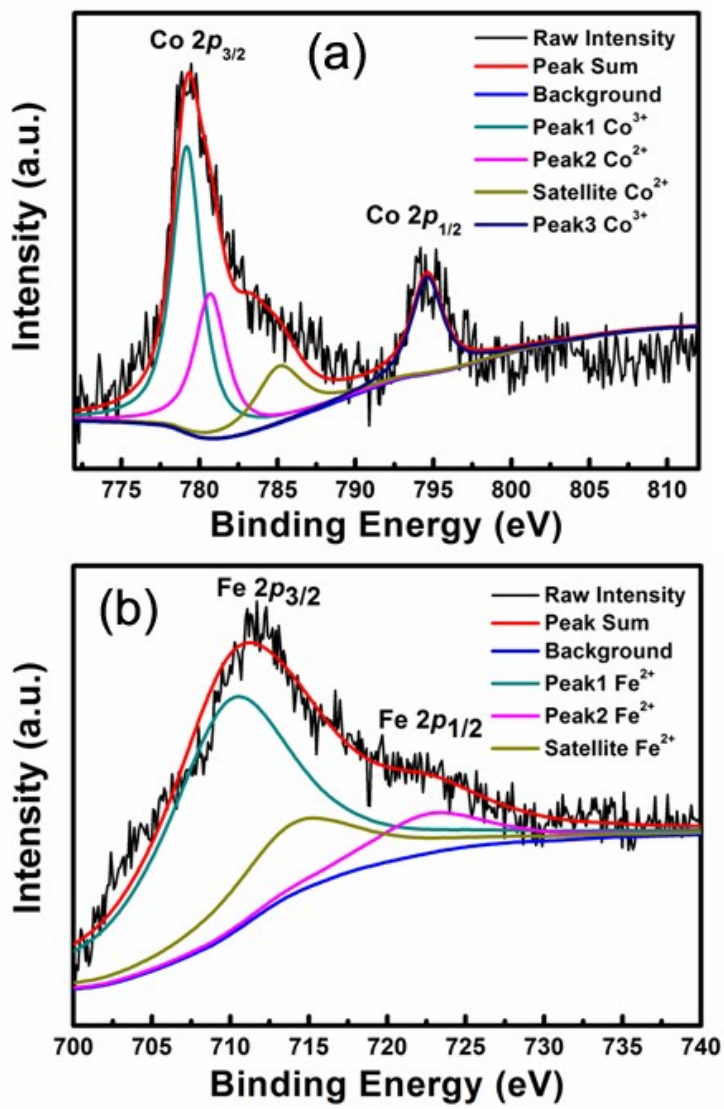

Fig. S2. XPS spectra of the $FeCo_2O_4$ on Ni foam: In the high-resolution Fe2*p* XPS spectrum (a), three peaks are observed at 709.9, 714.1 and 722.6 eV, indicating the presence of Fe^{2+}. In the Co2*p* XPS spectrum (b), five peaks reside at 779.2, 780.7, 785.1, 794.6 and 801.7 eV, which indicates that Co^{2+} and Co^{3+} exist together.[1,2]

References:

1. S. G. Mohamed, C. J. Chen, C. K. Chen, S. F. Hu and R. S. Liu, *ACS Appl. Mater. Interfaces*, 2014, **6**, 22701.
2. Y. Sharma, N. Sharma, G. V. S. Rao and B. V. R. Chowdari, *Solid State Ionics*, 2008, **179**, 587.

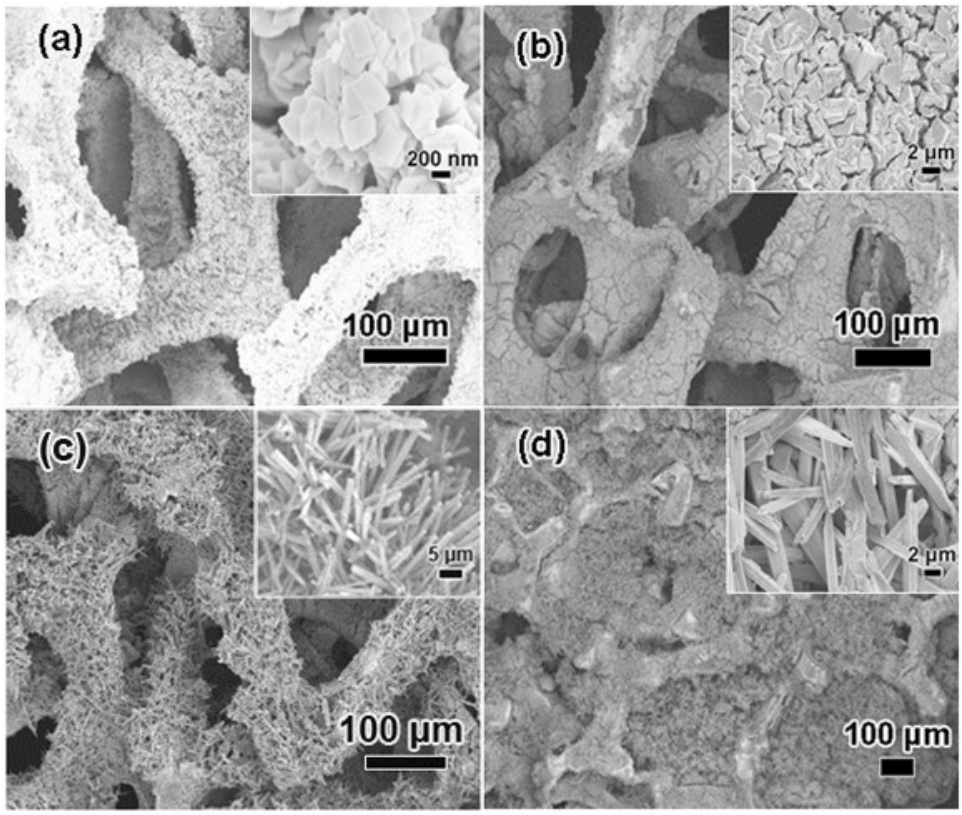

Fig. S3. SEM images of the $FeCo_2O_4$ grown on Ni foam obtained with different C_{Fe}^{3+} of (a) 1.3 mM (b) 5.0 mM (c) 12.5 mM (d) 17.5 mM.

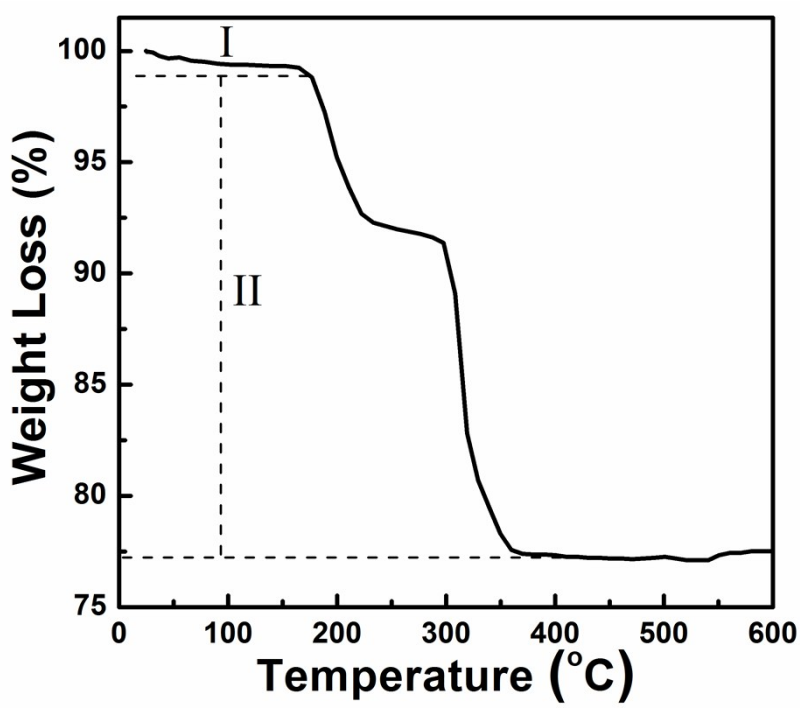

Fig. S4. TGA curve of a typical sample before thermal conversion, which was recorded from room temperature to 600°C.

The TGA curve of a typical sample (C_{Fe}^{3+} = 10 mM) before thermal conversion shows an initial mass loss due to the evaporation of water. The loss between 190°C to 350 °C (stage II) results from the decomposition. The $FeCo_2O_4$ content in this sample is thus 12.77 wt.%, and its mass density in the electrode 1.5 mg cm^{-2}.

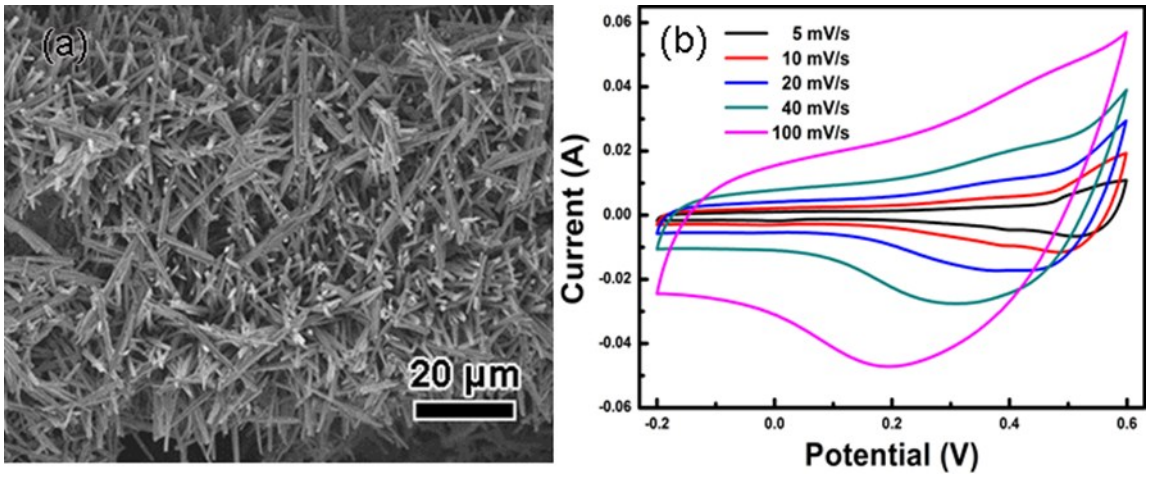

Fig. S5. SEM image (a) and CV curves (b) of typical $FeCo_2O_4$ tube arrays on Ni foam after ultrasound.

Table S1. Comparison of the optimal $FeCo_2O_4$ submicron tubes on Ni foam and previously reported ternary metal oxides of cobalt

Composites	Specific capacitance	Rate capability	Cycling stability	Reference
$FeCo_2O_4$ submicron tubes	1254 F/g at 2 mA/cm^2	73% from 2 to 100 mA /cm^2	91% after 5000	This work
$MnCo_2O_4$ nanoparticles	405 F/g at 5 mA/cm^2	67.9% from 4 to 40 mA/cm^2	95.1% after 1000	23
$CuCo_2O_4$ particles	338 F/g at 1 A/g	26% from 1 to 50 A/g	96% after 5000	5
$ZnCo_2O_4$ nanotubes	770 F/g at 10 A/g	84% from 10 to 60 A/g	89.5% after 3000	6
$NiCo_2O_4$ nanoparticles	726.8 F/g at 1 A/g	69% 1 to 20 A/g	72.7% after 2000	7
$NiCo_2O_4$ nanosheets	1002 F/g at 1 A/g	52% from 1 to 20 A/g	93% after 2000	24
$NiCo_2O_4$ nanosheets	1422 F/g at 1 A/g	70% from 1 to 20 A/g	84.4% after 3000	25
$NiCo_2O_4$ nanoparticles	1254 F/g at 2 A/g	54.1% from 1 to 20 A/g	70.4% after 1000	26